34th Annual International Conference of the IEEE EMBS
San Diego, California USA, 28 August - 1 September, 2012

Numerical and Experimental Characterization of Radiofrequency Ablation in Perfused Kidneys

Kristian Frank, Herbert Lindenborn and Dirk Dahlhaus
Communications Laboratory, University of Kassel, Germany
kristian_frank@student.uni-kassel.de, {lind,dahlhaus}@uni-kassel.de

Abstract— **We develop a three-dimensional finite element model in order to predict the resulting temperature distribution of a radiofrequency ablation (RFA) treatment in human kidneys. Here, a strong cooling effect results from a high degree of blood perfusion, which is modeled via two different approaches. The influence of big blood vessels for treatments close to renal hilus is modeled by including a cylindrical cooling tube based on the renal artery (or vein) in the kidney model. The influence of the perfusion of small arterioles and capillaries is represented by Pennes' approach in the bioheat equation. The experimental validation is performed by an in vivo RFA treatment on porcine kidney. Prior to the in vivo measurements several ex vivo experiments on fresh kidneys are carried out as a plausibility check for the model. During the treatments temperature profiles are measured using thermocouples which are radially arranged around the RFA applicator trocar. The evaluated data for each sensor show a deviation between 0.01 and 12 % from the simulation results. The approach serves for the design of a preplanning tool for RFA treatment in the future.**

I. INTRODUCTION

In recent years radiofrequency ablation (RFA) has become an accepted cancer therapy for patients who are contraindicated to surgery. For a RFA treatment an electrode positioned inside a tumor heats the cancerous tissue by applying an alternating current in the radiofrequency range in order to destroy the diseased area. Several types of so-called applicators differing in the number of electrodes or the chosen electric power profile (e.g. pulsed or constant) can be employed for this purpose. The placement of the applicator is usually controlled by imaging methods such as computerized tomography or sonography and can be applied percutaneously. Temperatures between approximately 50 and 100°C are adequate to destroy the diseased tissue [1]. At temperatures above 100°C carbonization effects occur which lead to an enormous rise in impedance and hence to an early termination of the treatment. To ensure a sufficient size of the necrosis area and protect adjacent healthy tissue against heating an accurate knowledge of the temperature distribution in the vicinity of the ablation region is essential. Main problems for the prediction of the necrosis area are complex morphologies of treated organs or a high degree of perfusion.

In this paper, we develop a three-dimensional finite element model in order to predict the resulting temperature distribution of a RFA treatment at 460 kHz in human kidneys where both aforementioned problems are addressed. The morphology of kidneys is quite complex with different types of tissue such as renal cortex, renal pyramids or fat. Furthermore, they are nerved by blood vessels of different sizes. Kidneys are organs with substantial perfusion of 1 - 1.25 l/min. In our approach we model the kidney as a homogeneous body of renal cortex. The physical model is described by a combination of partial differential equations for heat transfer, fluid dynamics and electromagnetic waves which are combined with equations for the dielectric properties of renal tissue. A multi-physics simulation serves for solving the equations and calculating the resulting space-time temperature distribution. The findings are compared to temperature measurements taken from an animal experiment in order to verify the model. The modeling of the cooling effect caused by blood perfusion deserves special attention where the perfusion can be seperated into two parts: Firstly, the influence of big blood vessels close to the ablation region and secondly, the perfusion of small vessels like arterioles and capillaries. Big blood vessels are modeled as a tube perfused by cooling blood close to the target area while the small vessels are taken into account by an additional term in the bioheat equation. The overall objective is to extend the approach in [2]-[4] to include blood perfusion in order to predict the temperature distribution in locations with big blood vessels where RFA is presently contraindicated.

The paper is organized as follows. Section II describes the methodology for modeling the system using a multi-physics approach. In Sect. III, the experimental validation using ex vivo and in vivo measurements is presented. In Sect. IV, the numerical solution of the multi-physics model is compared with the ex vivo and in vivo measurements. Conclusions are drawn in Sect. V. In this paper, boldface quantities indicate vectors and $\mathbf{a} \cdot \mathbf{b}$ is the inner product of the vectors $\mathbf{a}$ and $\mathbf{b}$.

II. METHODOLOGY

A. System description and modeling

We use an umbrella-shaped unipolar needle electrode with eight electrode arms and an umbrella diameter of 2 cm to introduce an alternating current at 460 kHz into renal tissue. The treated kidneys approximately have a length of 10 cm, a maximum width of 5 cm and a height of 3 cm. Therefore, the kidney model is generated as a cylindrical geometry in Fig. 1 having an elliptic footprint with a semi-major axis of 5 cm, a semi-minor axis of 2.5 cm and a height of 3 cm. The mesh in Fig. 1 arises from the finite-element method employed in Sect. IV for solving the system equations. Blood vessels like

978-1-4577-1787-1/12/$26.00 ©2012 IEEE

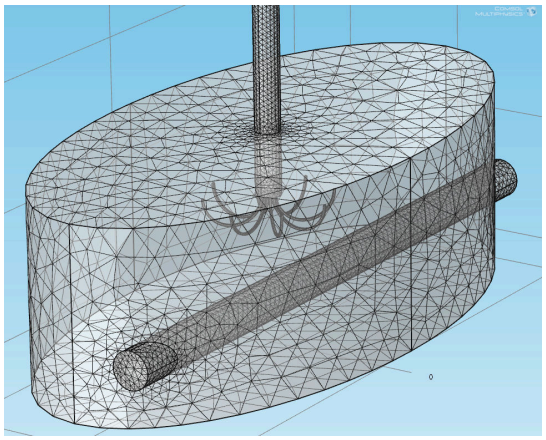

Fig. 1. Cylindrical structure: model of the kidney; vertical structure: applicator; horizontal structure: tube modeling blood vessels; finite element method with 145000 elements and 29000 nodes (cf. Sect. IV).

the renal artery are modeled as a horizontal tube of diameter 0.6 cm being asymmetrically positioned in the kidney. This arrangement is a reasonable model for treatments close to the renal hilus where big blood vessels enter or leave the kidney. For treatments far from the hilus, the tube in Fig. 1 is simply left out.

Renal tissue is considered to be an isotropic medium with non-homogeneous characteristics regarding its dielectric and thermal parameters. For simplicity, most parameters describing the model in Fig. 1 are assumed constant although they can be slowly time-variant or even depend on specific tissue effects on a molecular scale. Regarding these dependencies we implement a mathematical formulation which Pop et al. [5] have been able to derive for the change that dielectric parameters of porcine renal cortex undergo during a tissue heating using RFA with a radio frequency of 460 kHz. They suggest to decompose the time-temperature dependency into two independent effects, namely a reversible purely temperature depending effect given by a linear term and a non-reversible effect due to tissue denaturation which can be quantified by employing an Arrhenius model [5]. The expressions for the dielectric properties of renal tissue are described by the electric conductivity σ and the relative permittivity ε_r given by[1]

$$\sigma = \sigma_0\left[1+\sigma_1(T-T_0)+\Delta\sigma_{\max}(1-v(t,T))\right] \tag{1}$$

$$\varepsilon_\mathrm{r} = \varepsilon_{\mathrm{r}0}\left[1+\varepsilon_{\mathrm{r}1}(T-T_0)+\Delta\varepsilon_{\max}(1-w(t,T))\right], \tag{2}$$

where the functions $v(t,T)$ and $w(t,T)$ satisfy the differential equations

$$\frac{\partial v(t,T)}{\partial t} = -A_\sigma \exp\left(-\frac{E_{\mathrm{a},\sigma}}{RT(t)}\right) v(t,T) \tag{3}$$

$$\frac{\partial w(t,T)}{\partial t} = -A_\varepsilon \exp\left(-\frac{E_{\mathrm{a},\varepsilon}}{RT(t)}\right) w(t,T). \tag{4}$$

[1]A neglect of the Arrhenius term in (1) and (2) leads to a decrease of the final temperature in the simulation by about 1 degree, cf. Fig. 6.

Here, σ_0, σ_1, $\varepsilon_{\mathrm{r}0}$ and $\varepsilon_{\mathrm{r}1}$ are the zeroth and first order temperature coefficients, while $\Delta\sigma_{\max}$ and $\Delta\varepsilon_{\max}$ are the maximum changes of dielectric parameters calculated by means of the difference of completely denaturated state and native state values [5]. Furthermore, A_σ and A_ε are the frequency constants in each case, $E_{\mathrm{a},\sigma}$ and $E_{\mathrm{a},\varepsilon}$ the corresponding activation energies, R is the gas constant and T_0 is the ambient temperature which is assumed to be 22 °C in [5].

For the thermal conductivity k of porcine renal cortex a linear approximation regarding its temperature dependence can be found in [6] where the zeroth order and first order temperature coefficients k_0 and k_1, resp., are determined by several in vitro measurements between 3 and 45 °C according to

$$k = k_0 + k_1 T. \tag{5}$$

All other parameters are considered to be constant. The blood's thermal parameters ρ_{bl}, c_{bl}, k_{bl} and the electric conductivity σ_{bl} are taken from [7].

B. Physical Modeling

The heating effect caused by electromagnetic power dissipation is based on two different phenomena, namely the interaction $\mathbf{E}\cdot\mathbf{J}$ of the electric field $\mathbf{E}$ and the conduction current density $\mathbf{J}$ and the interaction $\mathbf{E}\cdot\frac{\partial\mathbf{P}}{\partial t} = \mathbf{E}\cdot\mathbf{J}_{\mathrm{pol}}$ of the electric field and the temporal changes of the polarization. Here, $\mathbf{J}_{\mathrm{pol}} = \frac{\partial\mathbf{P}}{\partial t}$ is the polarization current density. The changes of polarization are caused by a displacement current density $\frac{\partial\mathbf{D}}{\partial t}$, where $\mathbf{D}$ is the electric flux density. With the permittivity of free space $\varepsilon_0 = 8.854\cdot10^{-12}$ F/m and the assumption of an isotropic medium, where the polarization is given by $\mathbf{P} = \mathbf{D} - \varepsilon_0\mathbf{E}$ the total electromagnetic heat source Q_{em} reads

$$Q_{\mathrm{em}} = \mathbf{E}\cdot(\mathbf{J}+\mathbf{J}_{\mathrm{pol}}) = \mathbf{E}\cdot(\sigma\mathbf{E}+\varepsilon_0\frac{\partial}{\partial t}((\varepsilon_\mathrm{r}-1)\mathbf{E})).$$

This equation quantifies the influence of the dielectric parameters on the resulting tissue heating effect. If the wavelength of the electromagnetic excitation is much larger than the dimensions of the considered geometry, the simplification of magnetoquasistatics, where the displacement current is neglected, can be used. Since in renal tissue the effective wavelength for 460 kHz is about 10 m, the assumption of magnetoquasistatics can be considered valid[2]. Here, the whole set of equations reads

$$\nabla\cdot\mathbf{J} = 0 \tag{6}$$

$$\mathbf{J} = \sigma\mathbf{E} \tag{7}$$

$$\mathbf{E} = -\nabla V, \tag{8}$$

[2]If we do not neglect the displacement current and solve the arising equations in a similar fashion as described here, the temperature deviation as compared to the case of magnetoquasistatics is negligible, but the computation time in corresponding simulations is substantially increased. Therefore, at a frequency of 460 kHz, the approximation of magnetoquasistatics represents a good trade-off between systematic errors and model complexity.

where the scalar electric potential V on the electrodes is given by the root mean square of the applied sinusoidal voltage. The temperature and electromagnetic field quantities are coupled in (7) via the temperature dependent σ in (1) and the bioheat equation

$$\rho c_{\mathrm{p}} \frac{\partial T}{\partial t} + \rho c_{\mathrm{p}} (\mathbf{v} \cdot \nabla) T = \nabla \cdot (k \nabla T) + Q_{\mathrm{em}} - Q_{\mathrm{bio}} \qquad (9)$$

with $Q_{\mathrm{bio}} = \rho_{\mathrm{bl}} c_{\mathrm{bl}} \omega_{\mathrm{bl}} (T(t) - T_{\mathrm{bl}})$, where ρ is the density of the material, c_{p} the specific heat and $\mathbf{v}$ the vector of blood velocity inside the big blood vessel, respectively. The term Q_{bio} represents the cooling effect of the blood perfusion in the millions of very small blood vessels. Furthermore ω_{bl} is the blood perfusion rate in [1/s] which is estimated by averaging the whole blood perfusion of one kidney over the kidney volume and T_{bl} is the blood temperature of 37°C. Note that the electromagnetic heat source in (9), in view of the magnetoquasistatics assumption with $\frac{\partial \mathbf{P}}{\partial t} = \mathbf{0}$, reduces to $Q_{\mathrm{em}} = \mathbf{E} \cdot \mathbf{J}$. Here, (9) is to be seen as a polymorph representation of the bio-heat equation. The total derivative of the temperature T (left hand side of (9)) is only valid inside the blood vessel, in all other regions the convective term $\rho c_p (\mathbf{v} \cdot \nabla) T$ is neglected.

To define initial conditions it is assumed that the applicator temperature is identical to the temperature of its surrounding tissue, so the thermal initial conditions are set to 37°C for the whole area. On the outer boundaries the temperature is also set to 37°C and the potential is set to 0 V (except for the ex vivo measurements where due to the experimental set-up only the lower boundary is assumed to be grounded). The potential of the applicator is set to the values which have been determined by voltage metering during the experiments. Table 1 shows an overview of the different material parameters.

TABLE I

MATERIAL PARAMETERS

Parameter	Value	Dimension
σ_0	0.22	S/m
$\varepsilon_{\mathrm{r0}}$	3210	1
σ_1	$1.62 \cdot 10^{-2}$	S/(m·K)
$\varepsilon_{\mathrm{r1}}$	$1.31 \cdot 10^{-2}$	1/K
$\Delta\sigma_{\mathrm{max}}$	0.63	S/m
$\Delta\varepsilon_{\mathrm{rmax}}$	-0.57	1
A_σ	$5.73 \cdot 10^{34}$	1/s
A_ε	$5.85 \cdot 10^{28}$	1/s
$E_{\mathrm{a},\sigma}$	$57.42 \cdot 10^{3}$	cal/mol
$E_{\mathrm{a},\varepsilon}$	$48.32 \cdot 10^{3}$	cal/mol
R	1.98	cal/(mol· K)
k_0	0.4967	W/(m·K)
k_1	0.001176	W/(m·K^2)
ρ_{bl}	1000	kg/m^3
c_{bl}	4180	J/(kg·K)
k_{bl}	0.543	W/(m·K)
σ_{bl}	0.667	S/m
ω_{bl}	0.047	1/s

The numerical solution of the aforementioned coupled partial differential equations taking into account spatial boundary and temporal initial conditions is based on a finite element method implemented using the software package COMSOL MULTIPHYSICS release 4.2a similar to the approach in [2]-[4].

III. EXPERIMENTAL SET-UPS

A. Ex vivo measurements in non-perfused kidneys

We heat fresh non-perfused porcine kidneys in a climate chamber to 37°C and measure the temperature profile during the RFA treatment with eight thermocouples according to the set-up in Fig. 2. The latter are positioned on two circles

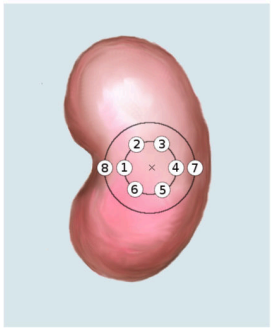

Fig. 2. Ex vivo set-up; cross-section of kidney with applicator stuck into the centre and eight thermocouples placed on two concentric circles around it.

around the applicator in the centre, where six sensors are placed on the inner circle with radius 1 cm and the remaining two sensors are placed on the outer circle with radius 2 cm. The needle shaped thermocouples stuck 1.5 cm into the kidney have a rectangular cross-section of 0.3×0.3 mm^2, which enables a precise positioning and low distortion of the temperature field, but also makes the sensors susceptible to bending. The umbrella-shaped electrode of diameter 2 cm is stuck 1 cm into the kidney and a plain counter electrode is placed below the kidney. The power is set to 5 W during a ten-minutes ablation process. This relatively low power is chosen in order to keep the maximum temperature below 100°C where carbonization effects are expected to occur. Furthermore, the temperature dependent formulations of the material parameters (1), (2) and (5) are not expected to be valid anymore for high temperatures around 100°C.

B. In vivo measurements in perfused kidneys

The in vivo measurements are carried out to take into account the perfusion and are done in cooperation with the department of urology at the university hospital of Dusseldorf, Germany. The treated pig is 4 years old and weighs 143 kg. The complete surgical intervention takes 4 hours. To reach the retroperitoneal positioned kidneys, parts of the gut need to be exposed and kept moist. The date of euthanasia is three days after surgery. This time period is necessary to evaluate usable data in the histological analysis. The same sensor arrangement which has been used for the ex vivo measurements in Fig. 2 is employed here. Fig. 3 shows how the applicator and the sensor arrangement is placed inside the pig's abdominal cavity. Here, the white, cylindrical device in the middle of the figure is the top of

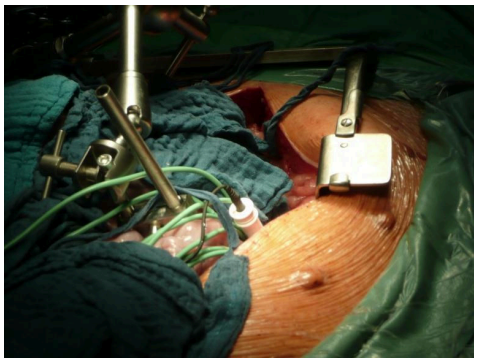

Fig. 3. Applicator and sensor positioning inside the pig's abdominal cavity.

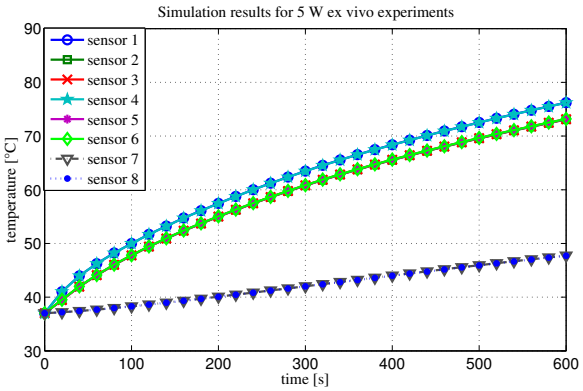

Fig. 4. Values of the simulated temperature profiles of ex vivo set-up.

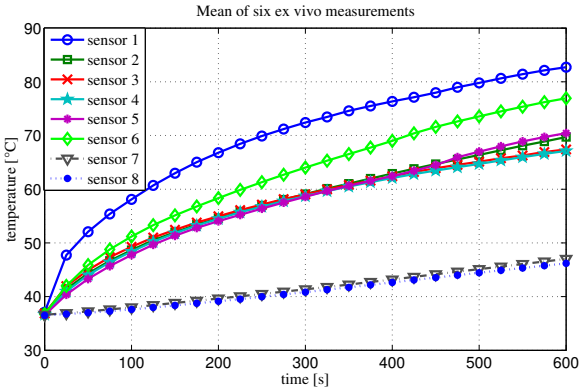

Fig. 5. Mean values of the temperature profiles of the six ex vivo measurements. The standard deviation for the respective sensors varies between approximately 1 and 7 °C.

the applicator trocar and the green wires around it connecting the sensors to the data logger. Along with the temperature, we also measure the impedance between the applicator and the counter electrode. Abrupt changes of the impedance indicate carbonization of the tissue, so the impedance serves as an indicator function. Since we want to keep temperatures below 100°C, we start the treatment with an excitation of 5 W. Then the power is increased by 5 W after 5, 11 and 15 minutes, so the power for the last 5 minutes of the ablation process is 20 W. The measured impedance varies between 51 and 49 Ω. We start a second ablation period where we focus on the maximum amount of power we can apply to keep below critical temperatures. Here we can achieve stable conditions (impedance of 49 Ω) with a power up to 50 W (over 5 minutes). The next step to 60 W leads to a rapid increase in impedance indicating a carbonization of the tissue close to the electrodes and subsequently an automatic abortion of the treatment is triggered. The rectally measured body temperature of the pig is 34.6°C. During the treatment four out of the eight sensors have been bent which leads to a substantial deviation of the corresponding temperature measurements. Therefore, we neglect these measurements in Sect. IV.

IV. Results

First, we investigate the temperature profiles simulated for the ex vivo set-up in Fig. 4. Here, the eight applicator electrodes are distributed regularly on a circle of diameter 2 cm such that two electrodes have identical azimuth angles at the thermocouples' positions 1 and 4 while the minimum azimuth angle deviation of thermocouples' positions 2, 3, 5, 6 and the applicator electrodes is 15° for each sensor. As expected from the symmetric sensor positions 7 and 8 in Fig. 2, the corresponding temperature characteristics are the same and lower than the temperatures for the thermocouples' positions on the inner circle. Similarly, the thermocouples' positions 2, 3, 5 and 6 show identical temperatures. The highest temperatures are observed at thermocouples' positions 1 and 4 which is due to the proximity of the applicator electrodes.

In Fig. 5, we show the corresponding *mean* values of temperature profiles measured in experimental ex vivo set-ups for six kidneys. Here, the measurements of thermocouples 7 and 8 are in good correspondence with the simulation results in Fig. 4. The measurements of thermocouples 1 - 6 show a deviation of approximately 2.5 - 9°C compared to the simulated values of corresponding sensors in Fig. 4. An additional analysis not discussed here shows that the temperature deviation is highly sensitive to a misplacement of the sensors. Therefore, in general, averaging over only *six* measurements is not sufficient to reduce significantly the observed deviations arising from sensor misplacements. The highest deviation of the temperature characteristics[3] in Fig. 4 and Fig. 5 is 9°C for sensor 4 corresponding to about 13.5 % of the maximum temperature 67°C in Fig. 5 reached after 10 minutes.

In Fig. 6 the results of the four correctly placed sensors of the in vivo measurement are shown and directly compared to the corresponding simulation results. We observe an excellent match for the temperature characteristics for thermocouples 4 and 7 with the simulated temperatures, while the deviations for thermocouple 6 are about 3°C and for thermocouple 3 about 5°C, respectively. Fig. 7 shows the percentage deviation of simulation and measurement results for each sensor.

[3]The percentage is calculated as the ratio of the temperature deviation and the measured temperature where both quantities are in centigrade.

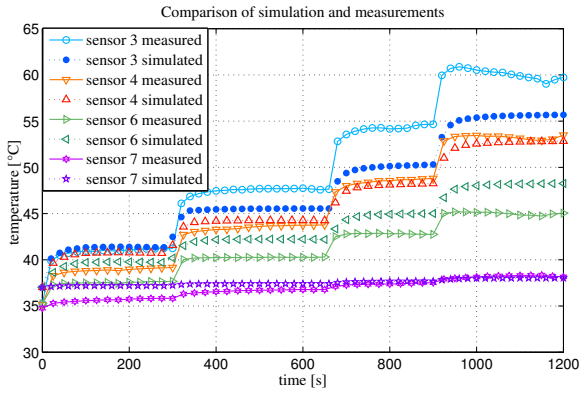

Fig. 6. Comparison of in vivo measurements and simulation results.

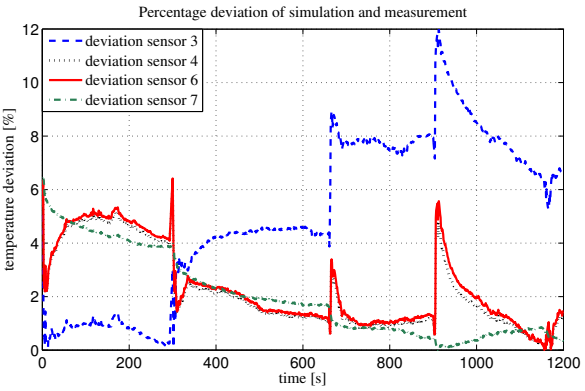

Fig. 7. Percentage deviation for the in vivo measurement.

Apart from the analysis of the deviations between simulation and experiment, the results of the in vivo measurement show a rapid saturation effect of the temperature for every step of power increase. This is expected to be a consequence of the strong perfusion of arterioles and capillaries. The comparison with the simulation results shows a good agreement for the rise time of the saturation effect. The percentage deviation in Fig. 7 for the four sensors is between 0.01 and 12 %. The achieved temperatures on the inner radius are between 45 and 61°C and around 38°C for sensor 7 on the outer radius. This shows that the power of 20 W has been chosen too low to cause necrosis in a distance of 2 cm from the trocar.

The in vivo measurements of the four sensors show a cooling effect caused mainly by the average cooling term Q_{bio} in (9), while cooling due to big blood vessels would require sensor measurements in the vicinity of the hilus, i.e. close to thermocouple 8. Unfortunately, the latter has been bent in the experimental set-up and thus not used for the analysis so that no direct proof of the cooling effect by big blood vessels could be given. However, the effect can be observed in the simulation. To that end, Fig. 8 shows the three-dimensional simulated isothermal surface of 45°C in a kidney of height 3 cm resulting from a 20-minutes treatment with the aforementioned power profile. The blood vessel represented by the tube in the left lower part of the figure leads to a distortion of the isothermal surface due to cooling.

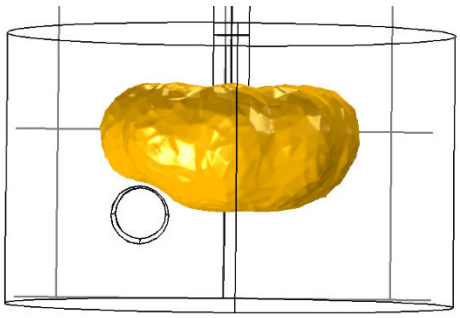

Fig. 8. Isothermal surface in a kidney with cooling effect caused by a big blood vessel in the lower left part of the kidney.

V. Conclusions

It has been shown that a model combining partial differential equations for heat transfer, fluid dynamics and electromagnetic waves is a suitable approach to describe temperature characteristics in radiofrequency ablation treatment of kidneys with complex morphology and high degree of perfusion. It has been shown by a comparison of in vivo experimental temperature measurements and numerical integration based on a finite element method that the impact of the perfusion by millions of arterioles and capillaries on the temperature can be properly modeled by the bioheat equation as proposed in the literature. In particular, saturation effects arising from cooling due to perfusion can be described accurately by the simulation. It turns out that the simplifying assumptions made in magnetoquasistatics are a valid approach for the formulation of the electromagnetic problem at frequencies around 460 kHz. The investigations can serve as a first step towards the design of a preplanning tool for radiofrequency ablation treatment.

References

[1] D. Panescu, J. G. Webster, "Effects of changes in electrical and thermal conductivities on radiofrequency lesion dimensions," *IEEE/EMBS*, 1997.

[2] M. Meyer, "Mathematische Modellierung und messtechnische Untersuchung von Applikatoren zur Radiofrequenzablation in zeitvarianten Medien". *Communications Laboratory at the Department of Electrical Engineering and Computer Science at the University of Kassel, Germany*, 2006.

[3] H. Velte, S. Laabs, B. Hemmerlein, H. Lindenborn, F.-P. Kuhn, D. Dahlhaus, M. Heuser, P. Albers, "Entwicklung eines Preplanning-Computermodells zur Radiofrequenzablation von Nierentumoren," *Der Urologe*, vol. 46, no. 9, pp. 1177–1178, 2007.

[4] M. Meyer, H. Velte, H. Lindenborn, A. Bangert, D. Dahlhaus, P. Albers, "Radiofrequency Ablation of Renal Tumors Improved by Preoperative ex-Vivo Computer Simulation Model," *Journal of Endourology*, vol. 21, no. 8, pp. 886-890, Aug. 2007.

[5] M .Pop, A. Molckovsky, L. Chin, M. C. Kolios, M. A. S. Jewett and M. D. Sherar, "Changes in dielectric properties at 460 khz of kidney and fat during heating: importance for radio-frequency thermal therapy," *Institute of Physics Publishing*, July 2003.

[6] J. W. Valvano, "Bioheat Transfer," *http://users.ece.utexas.edu/ valvano/research/jwv.pdf*.

[7] S. Tungjitkusolmun, S. T. Staelin, D. Haemmerich, J.-Z. Tsai, H. Cao, J. G. Webster, F. T. Lee, Jr., D. M. Mahvi, V. R. Vorperian, "Three-Dimensional Finite-Element Analyses for Radio-Frequency Hepatic Tumor Ablation," *IEEE Transactions on Biomedical Engineering*, vol. 49, no. 1, Jan. 2002.